THE EFFECTS OF WATER-CUO NANOFLUID FLOW ON HEAT TRANSFER INSIDE A HEATED 2D CHANNEL

MOHSEN KHALILI NAJAFABADI[1] – GABRIELLA BOGNÁR[1, *] – KRISZTIÁN HRICZÓ[2]

[1]*University of Miskolc, Department of Machine and Product Design,*
3515 Miskolc-Egyetemváros,
femohsen@uni-miskolc.hu
[2]*University of Miskolc, Institute of Mathematics,*
3515 Miskolc-Egyetemváros,
mathk@uni-miskolc.hu
[*]*Correspondence: v.bognar.gabriella@uni-miskolc.hu*
https://orcid.org/0000-0002-4070-1376 (Bognár G.)
https://orcid.org/0000-0003-3298-6495 (Hriczó K.)

Abstract: The velocity distribution and heat transfer improvement in a two-dimensional channel filled with a water-CuO nanofluid is numerically studied. The nanofluid flow is assumed laminar and one-phase with Newtonian behaviour. Pure water is considered as the base fluid, and water-CuO nanofluid with four different volume fractions of CuO nanoparticles are examined. A constant heat source–sink is considered to cover the entire length of the bottom wall of the channel while the upper wall is assumed thermally insulated. The control volume technique is used to discretize the governing differential equations, and the SIMPLE algorithm is used to solve the velocity-pressure coupling. A CFD simulation is applied on nanofluid flow utilizing ANSYS FLUENT to solve the governing equations of the flow. The effects of nanoparticle volume fraction on the heat transfer, velocity profile, wall shear stress, skin friction coefficient, and Nusselt number along the channel have also been examined. The results confirm that the volume fraction of nanoparticles plays an important role in heat transfer enhancement and hydrodynamic behaviour of flow. The results are presented in figures and tables.

Keywords: Nanofluid, CFD, heat transfer enhancement, numerical method, channel, 2D

1. INTRODUCTION

Conventional fluids have restricted heat transfer potential due to their poor thermophysical properties such as thermal conductivity. Therefore, scientists have attempted to resolve these kinds of difficulties by enhancing the thermal properties of these fluids to achieve more advanced capabilities. The number of industrial demands that might benefit from improved heat transfer fluids is infinite, including applications in hot rolling, paper drying, biomedicine, food processing, nuclear reactors, and so on. As a result, several strategies have been used to improve the thermal properties of conventional fluids.

Dispersion of nanoparticles in a base fluid was one of the first approaches. In fact, thermal characteristics can be improved by adding particles of different materials with a better thermal conductivity than the base fluid [1]. For example, metal particles have a greater thermal conductivity than the base fluid in general. Stephen [2] was the first to develop this approach, which he invented the word nanofluid in enhancing thermal conductivity. Because of the extremely high specific surface area of nanoparticles, nanofluids have a significantly greater effective thermal conductivity, making them a promising candidate for heat transfer applications. This method of improving thermal properties has received a lot of attention in a variety of other applications and academia. The study of the thermal physical characteristics of nanofluids reveals that a variety of factors influence the nanofluid's final performance. Volume fraction, base fluid, nanoparticle size and shape, and particle movement patterns are among the characteristics.

Many studies have focused on the impact of different nanoparticle kinds on heat transfer. In the classic Blasius problem, Anuar [3] investigated the effects of Al_2O_3, CuO, and TiO_2 particles. Bognar et al. [4] investigated three types of nanofluids, such as alumina (Al_2O_3), titania (TiO_2), and magnetite (Fe_3O_4), in a base fluid of water for viscous nanofluid flow (Sakiadis flow). They concluded that the solid volume percentage has a big impact on fluid flow and heat transfer. When the three types of nanoparticles were compared, the Al_2O_3 had a much higher thermal conductivity. In another study, Bognar et al. [5] utilized similarity analysis and CFD simulation to examine a steady two-dimensional nanofluid flow along a flat surface. Three different nanofluids were studied theoretically and numerically. The impact of a small number of solid particles (up to 4% concentration) on flow and heat transfer properties was investigated. They concluded that when the volume fraction increases, the dimensionless temperature increases because of improved heat transfer. Furthermore, in nanofluid field, the volume fraction is one of the most important factors. Lee et al. [6] demonstrated that when the volume fraction increased, the thermal conductivity increased linearly. Khanafer [7] devised a two-dimensional model to investigate the heat transfer properties of nanofluids inside a frame. Congedo [8] investigated the natural convection flow for Al_2O_3-water nanofluid. Different approaches have been used to examine the solution of nanofluid challenges. Authors have employed the single phase technique in a variety of geometries in the literature, including flat plate, wedge, square channel, circular tube, and flow over cylinder [9], [10], [11].

According to the literature [12], lubricating oils containing nanoparticles (MoS_2, CuO, TiO_2, diamond, etc.) have increased load-carrying capacity, anti-wear, and friction-reduction qualities. These properties made nanofluids particularly appealing for cooling and/or lubricating applications in a variety of industries, including manufacturing, transportation, energy, and electronics, and so on. For example, in compared to water as an absorbing medium, some experimental findings show that using the nanofluid improves collector efficiency in a solar collector [13]. In this study, the influence of a CuO–water nanofluid as the working fluid, on the performance and efficiency of a flat-plate solar collector is experimentally studied. In another application in enhanced oil recovery (EOR), metal oxide nanoparticles (such as CuO,

Fe_2O_3, and NiO) were discovered to be effective in reducing the viscosity of heavy oil [14]. Another use for nanoparticles is to raise the density and viscosity of a gas that has been injected to an oil well for enhanced oil recovery [15]. In this technique, gas flooding mobility is efficiently controlled, improving gas displacement efficiency and oil recovery. On the EOR of heavy oil, for example, several CO_2 nanofluid (CuO nanoparticles saturated with CO_2) core flood studies are carried out. The findings indicate that due to swelling and displacement of heavy oil, the nanoparticles-CO_2 nanofluid recovered 71.30 percent of the heavy oil, which was 13.30 percent greater than a traditional CO_2 core flood. The process is that adding nanoparticles increases both the density and viscosity of CO_2. The viscosity of CO_2 nanofluids was found to be 140 times that of regular CO_2. Bognar and Hriczo [16] examined the ferrofluid flow boundary layer caused by a permeable stretching sheet. They examined the effects of the magnetic field, Reynolds number, and porosity on the velocity and heat fields. They concluded that increasing the stretching, porosity, and ferromagnetic parameter reduces skin friction and heat transfer coefficients. In another numerical study, Bognar and Hriczo [17] studied the steady two-dimensional boundary layer flow across an extending flat sheet in a water-based ferrofluid. In ferrofluid flows along nonlinearly stretched sheets, the effects of volume fraction of solid ferroparticles and non-uniform magnetic field on dimensionless velocity and temperature, as well as the skin friction coefficient and local Nusselt number, were investigated for three selected ferroparticles (magnetite, cobalt ferrite, and Mn-Zn ferrite). They concluded that when the volume fraction increases, the nanofluid flow slows and the temperature increases.

Eastman et al. [18] concluded that a nanofluid made up of water and 5% CuO nanoparticles can improve thermal conductivity by around 60%. Lee et al. [6] showed that CuO particles are smaller than Al_2O_3 particles, implying that CuO-nanofluids have higher thermal conductivity than Al_2O_3-nanofluids. Heris et al. [19] considered a constant temperature boundary condition rather than a constant heat flux condition by flowing saturated steam in a tube. They discovered that increasing the nanoparticle volume fraction and the Peclet number improves the heat transfer coefficient. However, as compared to CuO-water nanofluid, Al_2O_3-water nanofluid demonstrated better improvement in heat transfer coefficient. Sivakumar et al. [20], on the other hand, observed that CuO-water nanofluid had a higher heat transfer coefficient than Al_2O_3-water nanofluid due to the high thermal conductivity of CuO particles. This disagreement might be attributed to changes in the boundary condition, nanoparticle size, and model shape. According to another study, CuO nanoparticles had the highest relative thermal conductivity coefficient thanks to their maximum density, followed by Al_2O_3, ZrO_2, TiO_2, and SiO_2. Al_2O_3 nanoparticles are ranked second after CuO nanoparticles [21]. Peng et al. [22] examined the effect of adding CuO nanoparticles to R113 refrigerant on the flow boiling heat transfer performance of the nanorefrigerant (CuO + R113 combination) within a smooth channel. Their findings revealed that the nanorefrigerant's heat transfer coefficient was higher than that of pure refrigerant, with a maximum improvement of 29.7%. Lu et al. [23] investigated the effect of CuO nanofluids based on water on an open thermo

syphon used in a high-temperature evacuated tabular solar collector (HTC). Nanofluid enhanced the evaporator's thermal performance when compared to water, and it also improved the evaporating heat transfer coefficient by 30%. According to Peyghambarzadeh et al. [24], increasing the concentration of CuO/water nanoparticles improves the model's thermal performance. Zarringhalam et al. [25] observed that a slight amount of CuO nanoparticles in water improves the average heat transfer coefficient significantly. Chein et al. [26] investigated CuO/water and discovered that the thermal improvement obtained by adding nanoparticles to the base fluid is dependent on particle size, shape, Reynolds number, and particle volume percent. In another study, the computer simulation of natural convection in a two-dimensional square cavity filled with a water–CuO nanofluid was carried out [27]. The findings suggest that when the Rayleigh number and the percentage of nanoparticles increase, the heat transfer rate increases independent of the position of the source-sink. These researches show that the presence of nanoparticles in the base fluid improves heat transfer.

The velocity distribution and heat transfer improvement of water-CuO nanofluid in a laminar 2D flow within a horizontal channel are investigated numerically in this study. The influence of the volume fraction on heat transfer, velocity, wall shear stress, skin friction coefficient, and Nusselt number have also been studied along the channel. The model is explained in section 2 along with the governing equations that describe the model. In section 3, the geometry generated, the mesh independency study, and the numerical solution method are presented. Finally, the results are presented in section 4.

2. MODEL DESCRIPTION AND GOVERNING EQUATIONS

2.1. Model description

Figure 1 demonstrates the geometry and the computational domain schematically. The channel's diameter and length have been set at 0.1 m and 2 m, respectively. With a temperature of 275 K and a velocity given by Reynolds numbers equal to 1,000 (Re = 1,000), the flow at the inlet has been assumed to be hydrodynamically steady. The lower wall receives a constant heat flux of 200 W/m^2 from downside, while the upper wall is set to be adiabatic from up. This numerical investigation uses a single-phase technique to solve the nanofluid flow problem. The following assumptions are employed in this approach:

1. The nanoparticles and the base fluid (water) are assumed to be mixed precisely and the whole mixture is regarded homogeneous. In addition, the fluid phase and solid particles are supposed to be in thermal equilibrium and to flow at the same speed.
2. Fluid flow that is steady, Newtonian, and incompressible is considered.
3. The thermophysical properties of nanofluids, such as density, thermal conductivity, viscosity, and thermal conductivity, are temperature independent and completely depend on the nanoparticle volume fraction.
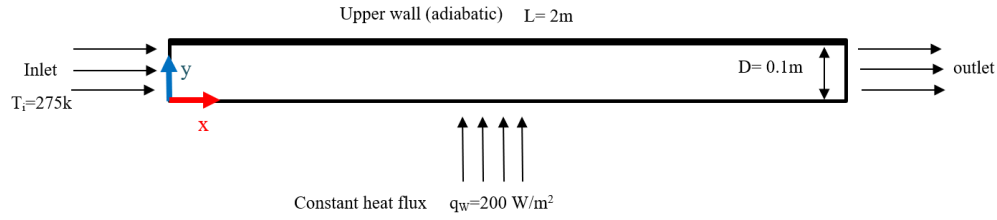
Figure 1. *The schematic diagram of the computational domain*

The wall is made from aluminium and its properties are given in *Table 1*.

<div align="right">Table 1</div>

Properties of wall made from aluminium

Density, ρ (kg/m³)	Specific heat, Cp (J/kg K)	Thermal conductivity, k (W/m K)
2,719	871	202.4

2.2. Governing equations

The mathematical formulation of the single-phase model for Newtonian fluid is presented by *Equations (1)* to *(3)*, which are continuity, momentum, and energy governing equations, respectively [28]:

$$\text{div}(\rho_{nf}\vec{V}) = 0, \tag{1}$$

$$\text{div}(\rho_{nf}\vec{V}\vec{V}) = -\nabla P + \mu_{nf}\nabla^2\vec{V}, \tag{2}$$

$$\text{div}(\rho_{nf}\vec{V}C_{pnf}T) = \text{div}(k_{nf}\nabla T). \tag{3}$$

The following notations are used in the above equations:
$\vec{V}$: the velocity vector,
P: the pressure of the nanofluid,
T: the temperature of the nanofluid,
μ_{nf}: the dynamic viscosity of the nanofluid,
ρ_{nf}: the density of the nanofluid is density of the nanofluid,
k_{nf}: thermal conductivity of the nanofluid,
Cp_{nf}: thermal capacity of the nanofluid.

2.3. Thermal properties of the nanofluid

As a function of the volume fraction, the thermal properties of the nanofluid are calculated. By using *Equations (4)–(7)*, the density, thermal capacity, viscosity, and thermal conductivity are estimated based on the concentration of nanoparticles in the base fluid. The effective density of the nanofluid is given by [29]:

$$\rho_{nf} = (1 - \varphi)\rho_{bf} + \rho_s\varphi, \tag{4}$$

where, ρ_{bf} and ρ_s refer to the density of base fluid and nanoparticles, respectively. The heat capacity of the nanofluid C_{pnf} is considered to be as below [29], [30]:

$$C_{pnf} = \frac{\varphi(\rho C_p)_s + (1-\varphi)(\rho C_p)_{bf}}{\rho_{nf}}. \tag{5}$$

The viscosity of nanofluid μ_{nf} is obtained from below equation, which is called Brinkman equation as follows [31], [32]:

$$\mu_{nf} = \frac{\mu_{bf}}{(1-\varphi)^{2.5}}, \tag{6}$$

where, μ_{bf} is the viscosity of the base fluid (water), and φ refers to nanoparticle volume fraction.

The thermal conductivity of nanofluid knf is given as follows [33]:

$$k_{nf} = k_{bf} \frac{k_s + 2k_{bf} - 2\varphi(k_{bf} - k_s)}{k_s + 2k_{bf} + \varphi(k_{bf} - k_s)}. \tag{7}$$

where, k_{bf} is the thermal conductivity of base fluid, and k_s is the thermal conductivity of the nanoparticles.

Thermo-physical properties for pure water and various types of nanoparticles are given in *Table 2*, and the thermo-physical properties for CuO-water nanofluid at different values of φ are presented in *Table 3*.

Table 2
Thermo-physical properties for pure water and
various types of nanoparticles [34]

PARTICLE TYPE	ρ (kg/m^3)	μ (N s/m^2)	k (W/m K)	Cp (J/kg K)
Pure water	998.2	0.001003	0.6	4,182
Al$_2$O$_3$	3,970	–	40	765
CuO	6,500	–	20	535.6
SiO$_2$	2,200	–	1.2	703
ZnO	5,600	–	13	459.2

Table 3
Thermo-physical properties for CuO-water at different values of φ
[29],[30],[31],[32], [33]

VOLUME FRACTION (φ)	(1%)	(2%)	(3%)	(4%)
ρ_{nf} (kg/m^3)	1,053.218	1,108.236	1,163.254	1,218.272
C_{pnf} (J/kg K)	3,956.96017	3,754.264391	3,570.74227	3,403.796118
k_{nf} (W/m K)	0.616623822	0.633557563	0.650809972	0.668390129
μ_{nf} (N s/m^2)	0.00102852	0.001054959	0.00108236	0.001110767

3. NUMERICAL PROCEDURE

3.1. Geometry and mesh independency investigation

The geometry is generated by using DesignModeler of official Ansys Fluent, and the two-dimensional flow problem in one-phase was selected. The channel's diameter and length have been set at 0.1 m and 2 m, respectively. The inlet flow temperature was set at 275 K with a velocity given by Reynolds numbers equal to 1,000. The lower wall receives a constant heat flux of 200 W/m^2, while the upper wall is set to be adiabatic. Non-uniform quadrilateral grid system is employed for meshing the domain generated by Meshing of official Ansys Fluent as shown in *Figure 2*. Because the accuracy of finite volume techniques is strongly related to the quality of the discretization utilized, the grid independence test is performed to confirm that the given solution is mesh independent. As a result, a precise mesh sensitivity investigation was conducted in order to reduce the numerical impacts imposed by mesh size. The mesh sensitivity was examined for six meshes, and the test compared the average Nusselt number on the bottom wall for each mesh. The results are shown in *Table 4*. The Nusselt number for mesh 3 with 12,400 cells was determined to be adequate for ensuring the accuracy of the solution as well as the grid's independence.
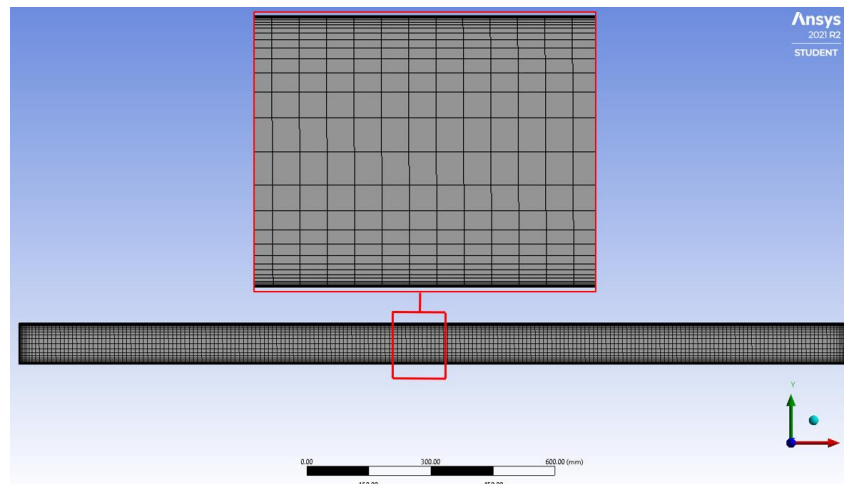

Figure 2. *Mesh generation for the model*

Table 4
Mesh independency investigation

Mesh	Number of cells	Average Nusselt number
1	2,400	23.88086
2	6,390	24.15811
3	**12,400**	**24.25852**
4	20,250	24.30758

3.2. Numerical solution method

The equations of mass, momentum, and energy were discretized using the finite volume method (FVM). The calculations were done using Ansys Fluent Solver, which solved the system of *Equations (1)–(3)* as well as the boundary conditions. The procedure for solving the problem was as follows: A simple algorithm was used to resolve the velocity-pressure coupling. The convection and diffusion terms in the governing equations were discretized using a second-order upwind scheme. The convergence criteria of the solutions monitored by a residual monitor of 10^{-6}.

4. RESULTS

4.1. Contours

4.1.1. Temperature contour of cuo-water nanofluid

The temperature contour for nanofluid containing 4% CuO along the whole channel is presented in *Figure 3*.
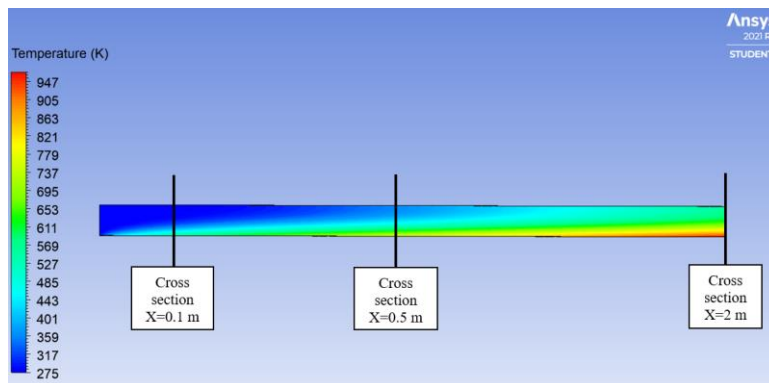
Figure 3. *Temperature contour for nanofluid containing 4% CuO along the pipe*
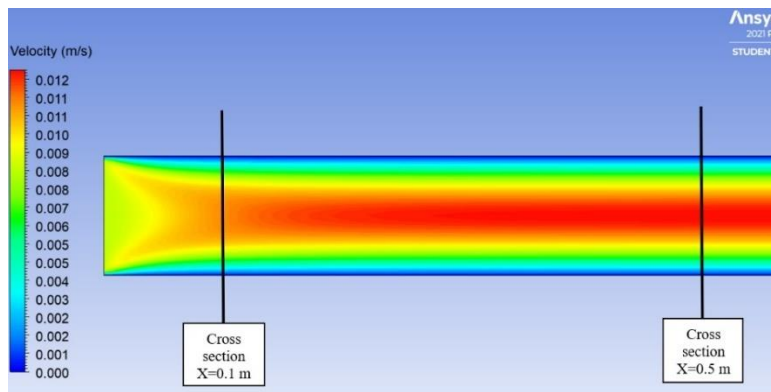

Figure 4. *Velocity contour for nanofluid containing 4% CuO along the pipe*

As it is illustrated, the nanofluid enters the channel at temperature equal to inlet temperature (275 K), and the temperature gradually increases as it moves forward along the channel. Due to having a constant heat flux at the lower wall while the upper wall is thermally insulated, the temperature of nanofluid at lower part of the channel specifically near to the lower wall tends to rise. To precisely investigate the thermal behavior of nanofluid, three cross sections along the channel (X = 0.1, 0.5, and 2 m) are selected and will be discussed in part 4.2.

4.1.2. Velocity contour of nanofluid containing cuo

The velocity contour for nanofluid containing 4% CuO along the section of the channel which a fully developed regime was established is presented in *Figure 4*. As it is illustrated, the velocity of nanofluid is not influenced by the thermal conditions at lower and upper walls, and it is only affected by the nanoparticle volume fraction. It is shown that the velocity near the walls is equal to zero due to no slip condition between walls and nanofluid. The velocity distribution along the channel is worthwhile to be studied. Therefore, two cross sections along the channel (X = 0.1 and 0.5 m) are selected and will be discussed in part 4.3.

4.2. Thermal effect of nanofluid containing CuO

Numerical results for the thermal boundary layers at different locations along the channel are presented. *Figure 5* depicts the impact of nanoparticle volume fraction on the temperature profile for CuO-water nanofluid flow at three different cross sections (X = 0.1, 0.5, and 2 m) along the channel.
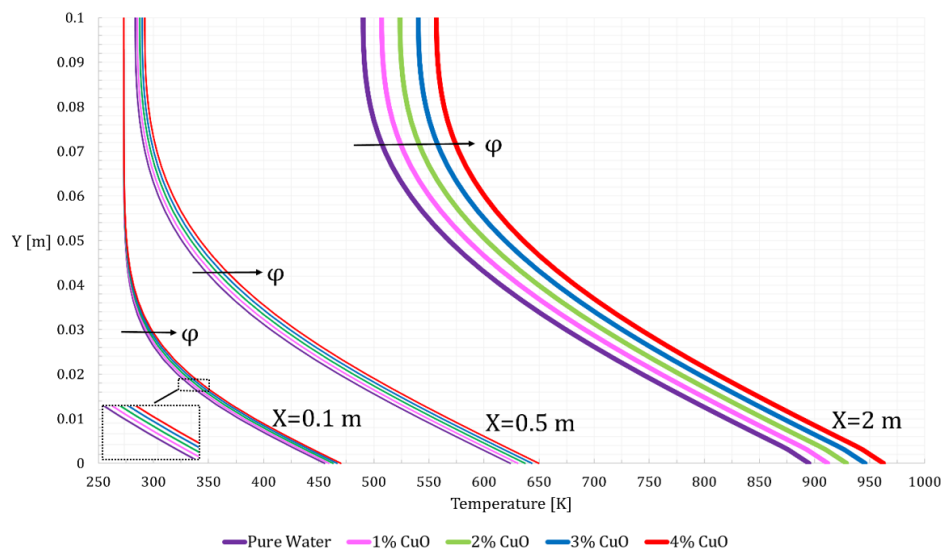

***Figure 5.** Temperature distribution at different cross sections for different nanoparticle volume fractions*

The Y-axis shows diameter of the channel while the X-axis shows temperature. Thermal boundary layer thickness increases with an increase in the parameter φ which is nanoparticle volume fraction. Comparison of the temperature profiles for different nanofluid concentrations shows that CuO-water at 4% has the thickest thermal boundary layer. Therefore, it is observed that the nanoparticles change the flow and heat transfer characteristics and causes an increase in the thermal boundary layer. Moreover, the graph shows that the temperature near the lower wall at cross section X = 0.1m is around 475 K while it rises to 650 K and 950 K at cross sections X = 0.5m and X = 2m, respectively. This is due to existence of a constant heat flux at the bottom wall along the channel when the nanofluid reaches the end of the channel, it receives more heat from the lower wall. However, the increase of temperature near the upper wall along the channel length is not as rapid as that of for the lower wall since the upper wall is thermally insulated and is receiving heat only from the nanofluid flowing inside the channel.

4.3. Hydrodynamic effect of nanofluid containing CuO

The velocity distributions of nanofluid for nanoparticle volume fractions φ = 1, 2, 3, and 4% of CuO with the inlet Reynold's number Re = 1,000 at cross sections X = 0.1m and X = 0.5 m along the channel are shown in *Figures 6–7*. The numerical simulations reveal that when the volume fraction increases, the velocity of nanofluid increases. Therefore, the volume fraction has an impact on the nanofluid's velocity, as shown by the results. It is shown that the maximum velocity of nanofluid happens at nanoparticle volume fraction equal to 4%. It can be observed from *Figure 6* that the velocity profile at cross section X = 0.1 has not arrived the fully developed regime yet; however, there is a fully developed regime at cross section X = 0.5 in *Figure 7*.
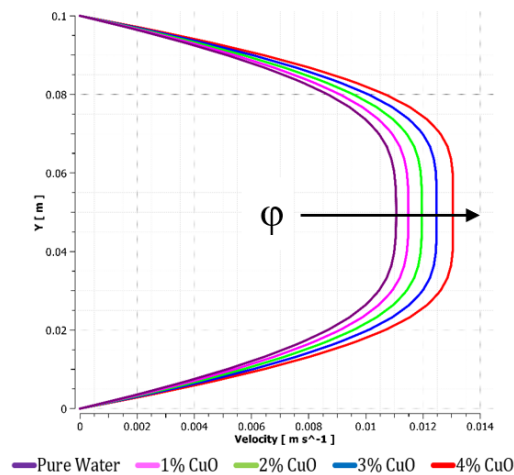

Figure 6. *Velocity distribution for different nanoparticle volume fractions at cross section X = 0.1 m*
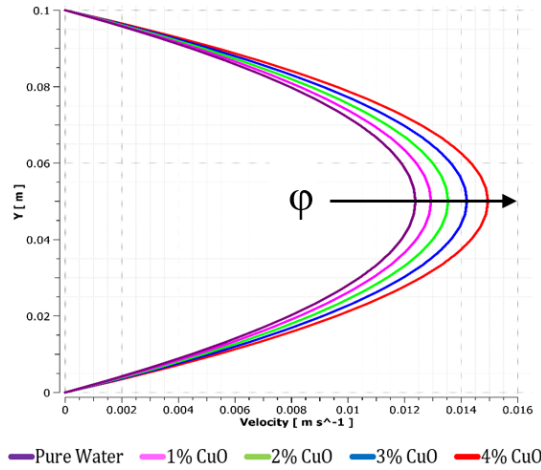
***Figure 7.** Velocity distribution for different volume fractions at cross section X = 0.5* m

The wall shear stress and skin friction coefficient are both of engineering importance and will be shown and examined in detail. The wall shear stress (τ_w) and heat flux (q_w) are defined as

$$\tau_w = \mu_{nf}\left(\frac{\partial u}{\partial y}\right)_{y=0}, \qquad q_w = -k_{nf}\left(\frac{\partial T}{\partial y}\right)_{y=0}, \tag{8}$$

while the skin friction coefficient (C_f) and the local Nusselt number (Nu) are defined as

$$C_f = \frac{\tau_w}{\rho_{nf}U^2}, \; Nu = \frac{x\,q_w}{k_{nf}(T_w - T_{nf})}. \tag{9}$$

Figure 8 shows the influence of the volume fraction on the wall shear stress along the channel's lower wall.
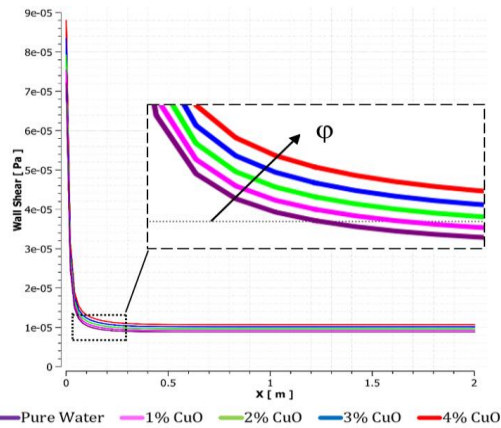

***Figure 8.** Wall shear stress at different volume fractions along the lower wall of pipe*

As it is shown, when the volume fraction of CuO nanoparticles increases, the value of the wall shear stress along the bottom wall increases. It shows that nanoparticle volume fraction has an impact on wall shear stress along the channel. Nanofluid with 4% of nanoparticle concentration has the highest amount of wall shear stress along the channel.

Figure 9 and *10* show the influence of the volume fraction on the skin friction coefficient and Nusselt number along the channel's lower wall. As it is shown, when the volume fraction of CuO nanoparticles increases, the value of the skin friction coefficient and Nusselt number along the bottom wall increases. It shows that nanoparticle volume fraction has an impact on skin friction coefficient and Nusselt number along the channel. Nanofluid with 4% of nanoparticle concentration has the highest amount of skin friction coefficient as well as Nusselt number along the channel.
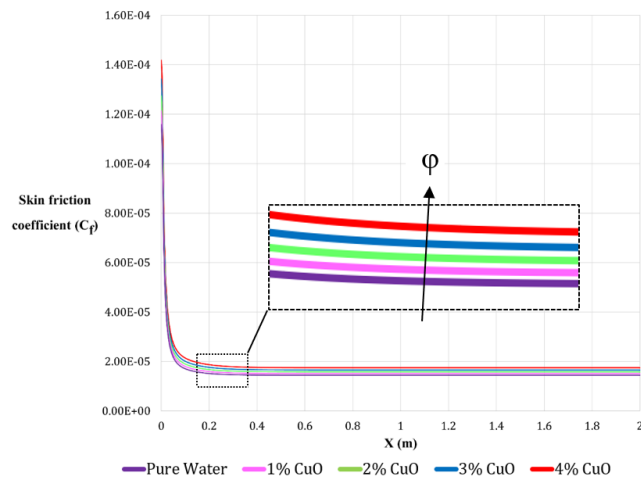

Figure 9. The skin friction coefficient at different volume fractions along
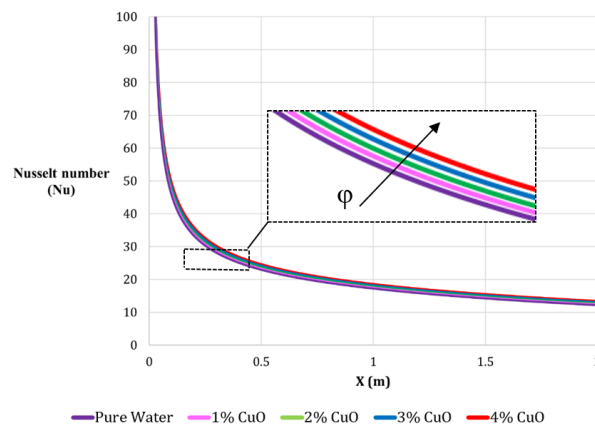the lower wall of pipe (it would be enough in the range of 0 and 8 10^{-5})

Figure 10. Nusselt number at different volume fractions along
the lower wall of pipe

5. CONCLUSION

Nanofluid flow within a horizontal channel was numerically investigated using CFD simulation. The influence of CuO nanoparticles on water base fluid has been highlighted in this work. It has been examined how the velocity distribution, the wall shear stress, skin friction coefficient, the temperature distribution, and Nusselt number vary with volume fraction of the nanoparticles. The maximum velocity shows an increase with increasing volume fraction. It is obtained that the temperature increased with increasing the volume fraction of CuO everywhere along the channel. Moreover, it is observed that when the volume fraction increases, the wall shear stress and skin friction coefficient, and Nusselt number along the channel increase as well. The goal is to see how the concentration of nanoparticles affects the velocity and temperature profiles of nanofluid flow in a horizontal channel. Further study is recommended in the transition and turbulent flow for the same model.

ACKNOWLEDGMENT

REFERENCES

[1] Hussein, A. M. – Bakar, R. A. – Kadirgama, K. – Sharma, K. V. (2013). Experimental measurement of nanofluids thermal properties. International Journal of Automotive and Mechanical Engineering, Vol. 7, No. 1. http://doi.org/10.15282/ijame.7.2012.5.0070

[2] Choi, S. U. S. (1995). *Enhancing thermal conductivity of fluids with nanoparticles*. American Society of Mechanical Engineers, Fluids Engineering Division (Publication) FED, Vol. 231. No. 1995.

[3] Anuar, N. S. – Bachok, N. (2016). Blasius and Sakiadis Problems in Nanofluids using Buongiorno Model and Thermophysical Properties of Nanoliquids. *European International Journal of Science and Technology*, Vol. 5, No. 4.

[4] Bognár, G. – Klazly, M. – Hriczó, K. (2020). Nanofluid flow past a stretching plate. *Processes*, Vol. 8, No. 7, 827, https://doi.org/10.3390/pr8070827.

[5] Bognár, G. – Klazly, M. – Mahabaleshwar, U. S. – Lorenzini, G. – Hriczó, K. (2021). Comparison of Similarity and Computational Fluid Dynamics Solutions for Blasius Flow of Nanofluid. *Journal of Engineering Thermophysics*, Vol. 30, No. 3, pp. 461–475, http://doi.org/10.1134/s1810232821030103.

[6] Lee, S. – Choi, S. – Li, S. – Eastman, J. (1999). Measuring Thermal Conductivity of Fluids Containing Oxide Nanoparticles. *Heat Transfer*, Vol. 121, No. 1999, http://doi.org/10.1115/1.2825978.

[7]   Khanafer, K. – Vafai, K. – Lightstone, M. (2003). Buoyancy-driven heat transfer enhancement in a two-dimensional enclosure utilizing nanofluids. *International Journal of Heat and Mass Transfer*, Vol. 46, No. 19. http://doi.org/10.1016/S0017-9310(03)00156-X

[8]   Congedo, P. M. – Collura, S. – Congedo, P. M. (2009). Modeling and analysis of natural convection heat transfer in nanofluids. *2008 Proceedings of the ASME Summer Heat Transfer Conference*, HT 2008, Vol. 3. http://doi.org/10.1115/HT2008-56289

[9]   Bianco, V. – Nardini, S. – Manca, O. (2011). Enhancement of heat transfer and entropy generation analysis of nanofluids turbulent convection flow in square section tubes. *Nanoscale Research Letters*, Vol. 6, No. 1. http://doi.org/10.1186/1556-276X-6-252

[10] Yacob, N. A. – Ishak, A. – Pop, I. – Vajravelu, K. (2011). Boundary layer flow past a stretching/shrinking surface beneath an external uniform shear flow with a convective surface boundary condition in a nanofluid. *Nanoscale Research Letters*, Vol. 6, No. 1, http://doi.org/10.1186/1556-276X-6-314.

[11] Bianco, V. – Chiacchio, F. – Manca, O. – Nardini, S. (2009). Numerical investigation of nanofluids forced convection in circular tubes. *Applied Thermal Engineering*, Vol. 29, No. 17–18. http://doi.org/10.1016/j.applthermaleng.2009.06.019

[12] Verma, A. – Jiang, W. – Abu Safe, H. H. – Brown, W. D. – Malshe, A. P. (2008). Tribological behavior of deagglomerated active inorganic nanoparticles for advanced lubrication. *Tribology Transactions*, Vol. 51, No. 5. http://doi.org/10.1080/10402000801947691

[13] Moghadam, A. J. – Farzane-Gord, M. – Sajadi, M. – Hoseyn-Zadeh, M. (2014). Effects of CuO/water nanofluid on the efficiency of a flat-plate solar collector. *Experimental Thermal and Fluid Science*, Vol. 58. http://doi.org/10.1016/j.expthermflusci.2014.06.014

[14] Patel, H. – Shah, S. – Ahmed, R. – Ucan, S. (2018). Effects of nanoparticles and temperature on heavy oil viscosity. *Journal of Petroleum Science and Engineering*, Vol. 167, http://doi.org/10.1016/j.petrol.2018.04.069.

[15] Shah, R. D. (2009). App1ication of nanoparticle saturated injectant gases for EOR of heavy oils. *Proceedings SPE Annual Technical Conference and Exhibition*, Vol. 7, http://doi.org/10.2118/129539-STU.

[16] Bognár, G. – Hriczó, K. (2020). Ferrofluid flow in magnetic field above stretching sheet with suction and injection. *Mathematical Modelling and Analysis*, Vol. 25, No. 3, pp. 461–472, http://doi.org/10.3846/mma.2020.10837.

[17]   Bognár, G. – Hriczó, K. (2020). Numerical Simulation of Water Based Fer-rofluid Flows along Moving Surfaces. *Processes*, Vol. 8, No. 7, p. 830. http://doi.org/10.3390/pr8070830

[18]   Eastman, J. A. – Choi, U. S. – Li, S. – Thompson, L. J. – Lee, S. (1997). En-hanced thermal conductivity through the development of nanofuids. *Nanophase and Nanocomposite Materials II*, http://doi.org/10.1557/PROC-457-3.

[19]   Heris, S. Z. – Etemad, S. G. – Esfahany, M. N. (2006). Experimental investi-gation of oxide nanofluids laminar flow convective heat transfer. *Interna-tional Communications in Heat and Mass Transfer*, Vol. 33, No. 4. http://doi.org/10.1016/j.icheatmasstransfer.2006.01.005

[20]   Sivakumar, A. – Alagumurthi, N. – Senthilvelan, T. (2016). Experimental in-vestigation of forced convective heat transfer performance in nanofluids of Al2O3/water and CuO/water in a serpentine shaped micro channel heat sink. *Heat and Mass Transfer/Waerme- und Stoffuebertragung*, Vol. 52, No. 7. http://doi.org/10.1007/s00231-015-1649-5

[21]   Rudyak, V. Y. – Belkin, A. A. – Tomilina, E. A. (2010). On the thermal con-ductivity of nanofluids. *Technical Physics Letters*, Vol. 36, No. 7. http://doi.org/10.1134/S1063785010070229

[22]   Peng, H. – Ding, G. – Jiang, W. – Hu, H. – Gao, Y. (2009). Heat transfer characteristics of refrigerant-based nanofluid flow boiling inside a horizontal smooth tube. *International Journal of Refrigeration*, Vol. 32, No. 6. http://doi.org/10.1016/j.ijrefrig.2009.01.025

[23]   Lu, L. – Liu, Z. H. – Xiao, H. S. (2011). Thermal performance of an open thermosyphon using nanofluids for high-temperature evacuated tubular solar collectors. Part 1: Indoor experiment, *Solar Energy*, Vol. 85, No. 2. http://doi.org/10.1016/j.enconman.2013.04.010

[24]   Peyghambarzadeh, S. M. – Hashemabadi, S. H. – Chabi, A. R. – Salimi, M. (2014). Performance of water based CuO and Al2O3 nanofluids in a Cu-Be alloy heat sink with rectangular microchannels. *Energy Conversion and Man-agement*, Vol. 86, http://doi.org/10.1016/j.enconman.2014.05.013.

[25]   Zarringhalam, M. – Karimipour, A. – Toghraie, D. (2016). Experimental study of the effect of solid volume fraction and Reynolds number on heat transfer coefficient and pressure drop of CuO-Water nanofluid. *Experimental Thermal and Fluid Science*, Vol. 76. http://doi.org/10.1016/j.expthermflusci.2016.03.026

[26]   Chein, R. – Chuang, J. (2007). Experimental microchannel heat sink perfor-mance studies using nanofluids. *International Journal of Thermal Sciences*, Vol. 46, No. 1, http://doi.org/10.1016/j.ijthermalsci.2006.03.009.

[27] Aminossadati, S. M. – Ghasemi, B. (2011). Natural convection of water-CuO nanofluid in a cavity with two pairs of heat source-sink. *International Communications in Heat and Mass Transfer*, Vol. 38, No. 5. http://doi.org/10.1016/j.icheatmasstransfer.2011.03.013

[28] Alrashed, A. A. A. A. et al. (2018). The numerical modeling of water/FMWCNT nanofluid flow and heat transfer in a backward-facing contracting channel. *Physica B: Condensed Matter*, Vol. 537. http://doi.org/10.1016/j.physb.2018.02.022

[29] Khanafer, K. – Vafai, K. (2011). A critical synthesis of thermophysical characteristics of nanofluids. *International Journal of Heat and Mass Transfer*, Vol. 54, No. 19–20, http://doi.org/10.1016/j.ijheatmasstransfer.2011.04.048.

[30] Xuan, Y. – Li, Q. (2000). Heat transfer enhancement of nanofluids. *International Journal of Heat and Fluid Flow*, Vol. 21, No. 1. http://doi.org/10.1016/S0142-727X(99)00067-3

[31] Mahbubul, I. M. – Saidur, R. – Amalina, M. A. (2012). Latest developments on the viscosity of nanofluids. *International Journal of Heat and Mass Transfer*, Vol. 55, No. 4, http://doi.org/10.1016/j.ijheatmasstransfer.2011.10.021.

[32] Abu-Nada, E. (2008). Application of nanofluids for heat transfer enhancement of separated flows encountered in a backward facing step. *International Journal of Heat and Fluid Flow*, Vol. 29, No. 1, pp. 242–249. http://doi.org/10.1016/j.ijheatfluidflow.2007.07.001

[33] Kakaç, S. – Pramuanjaroenkij, A. (2009). Review of convective heat transfer enhancement with nanofluids. *International Journal of Heat and Mass Transfer*, Vol. 52, No. 13–14, http://doi.org/10.1016/j.ijheatmasstransfer.2009.02.006.

[34] Kherbeet, A. S. – Mohammed, H. A. – Salman, B. H. (2012). The effect of nanofluids flow on mixed convection heat transfer over microscale backward-facing step. *International Journal of Heat and Mass Transfer*, Vol. 55, No. 21–22, http://doi.org/10.1016/j.ijheatmasstransfer.2012.05.084.